

Theoretical Exploration of the Mechanism of Riboflavin Formation from 6,7-Dimethyl-8-ribityllumazine: Nucleophilic Catalysis, Hydride Transfer, Hydrogen Atom Transfer, or Nucleophilic Addition?

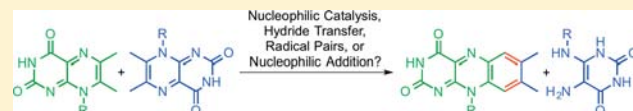
Martin Breugst,[†] Albert Eschenmoser,^{*,‡} and K. N. Houk^{*,†}

[†]Department of Chemistry and Biochemistry, University of California, Los Angeles, California 90095-1569, United States

[‡]Laboratory of Organic Chemistry, ETH Zürich, Hönggerberg Wolfgang-Pauli-Strasse 10, CHI H309, CH-8093 Zürich, Switzerland

S Supporting Information

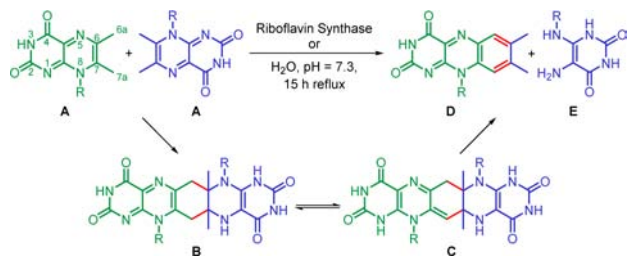
ABSTRACT: The cofactor riboflavin is biochemically synthesized by a constitutionally intricate process in which two molecules of 6,7-dimethyl-8-ribityllumazine react with each other to form one molecule of the cofactor and one molecule of 5-amino-6-(ribitylamino)uracil. Remarkably, this complex molecular transformation also proceeds non-enzymatically in boiling aqueous solution at pH 7.3. Four different mechanistic pathways for this transformation (nucleophilic catalysis, hydride transfer, hydrogen atom transfer, and a nucleophilic addition mechanism) have now been analyzed by density functional theory [M06-2X/def2-TZVPP/CPCM//M06-2X/6-31+G(d,p)/IEFPCM]. On the basis of these computational results, a so far unpublished nucleophilic addition mechanism is the lowest energy pathway yielding riboflavin. The previously proposed mechanism involving nucleophilic catalysis is higher in energy but is still a viable alternative for an enzyme-catalyzed process assisted by suitably positioned catalytic groups. Pathways involving the transfer of a hydride ion or of a hydrogen atom are predicted to proceed through higher energy transition states and intermediates.



INTRODUCTION

Riboflavin (**D**) plays a key role in metabolism and is required for a variety of cellular processes. In 1960, Plaut showed that two molecules of 6,7-dimethyl-8-ribityllumazine (**A**) are converted to one molecule of riboflavin (**D**) (Scheme 1).¹

Scheme 1. Enzyme-Catalyzed and Uncatalyzed Riboflavin Formation (R = d-Ribityl)



Isotopic labeling studies revealed that all four additional carbon atoms in **D** originate from the same lumazine derivative. Pyruvate, acetyl-CoA, or acetoacetate are not sources of the additional four-carbon atoms in riboflavin.² A few years later, 5-amino-6-(ribitylamino)uracil (**E**) was found to be the only byproduct in that reaction.³ **E** also happens to be one of the biosynthetic precursors of 6,7-dimethyl-8-ribityllumazine (**A**). Biosynthetically, the transformation shown in Scheme 1 is catalyzed by the enzyme riboflavin synthase.^{1–3} Under enzymatic conditions, the protons of the methyl group 7a attached to C-7 of the lumazine nucleus **A** (see Scheme 1 for

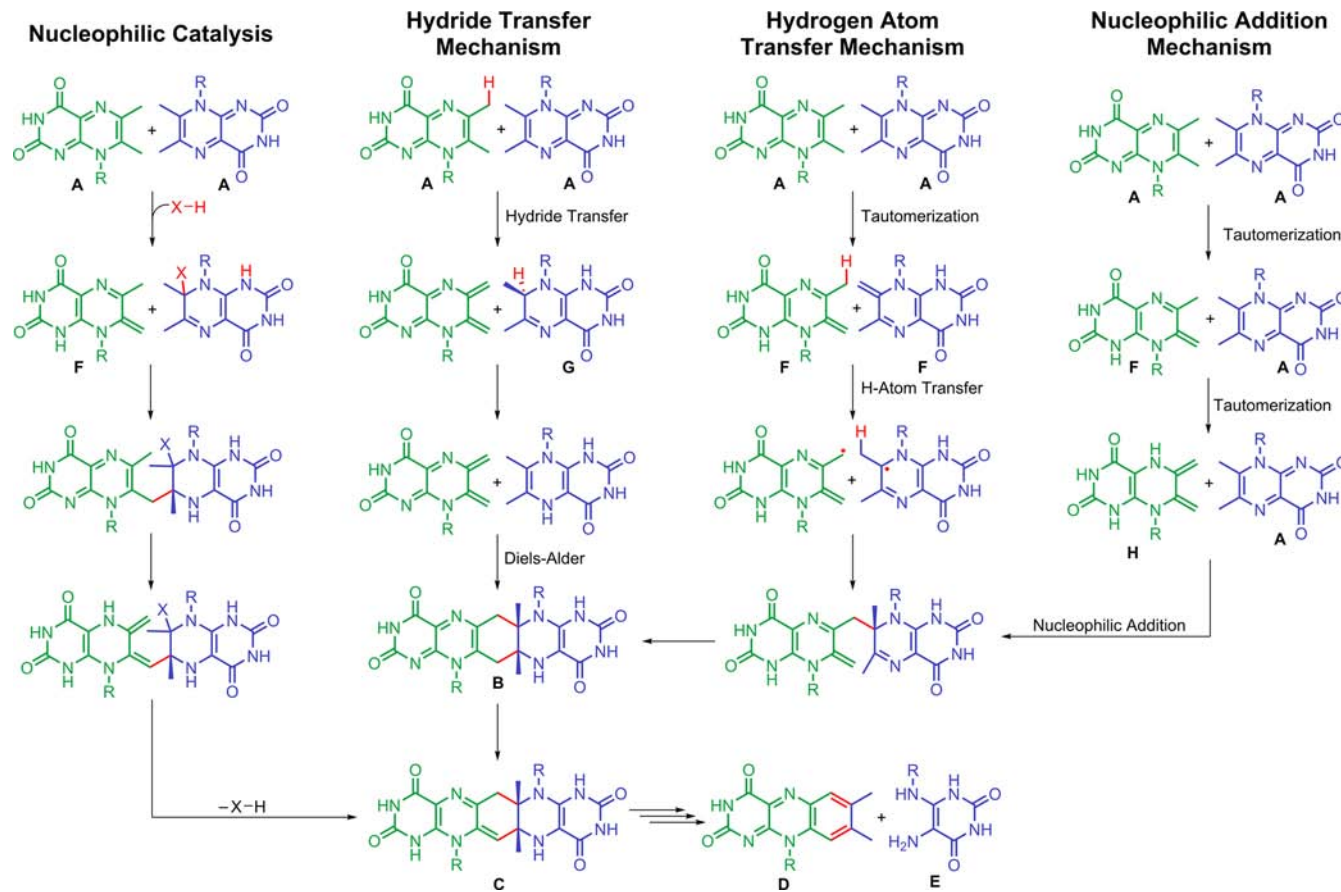
numbering) are freely exchangeable, and riboflavin formation starting from a substrate deuterated at the methyl group 6a at position 6 is strongly retarded.⁴ The overall reaction also takes place in the absence of the enzyme, in boiling water (phosphate buffer pH 7.3) under an inert atmosphere.⁵ Riboflavin synthase does not contain metal ions, prosthetic groups, or cofactors, and the enzymatic reaction only displays a moderate acceleration over the uncatalyzed reaction.⁶ Therefore, it has been proposed that the catalytic activity results from binding and properly aligning the substrate molecules.⁶

While animals and humans ingest riboflavin with food, many pathogenic bacteria including *Escherichia coli* or *Salmonella typhimurium* absolutely depend on an endogenous synthesis of **D**.⁷ As a consequence, inhibitors of riboflavin synthase should be toxic only for the microorganisms but not for the host and are therefore suitable targets for drugs with antibacterial activity.^{7b} For rational design of these inhibitors, a detailed picture of the mechanism of riboflavin formation is necessary. Despite such prospects and the importance of riboflavin in biochemistry and medicine, no generally accepted mechanistic pathway for this transformation has been established. Understanding this central step of riboflavin formation is also of interest to prebiotic chemistry because it represents an example of a central step in “chemomimetic” cofactor biosynthesis that does not necessarily require the assistance of an enzyme in order to proceed.

Received: February 27, 2013

Published: April 3, 2013



Scheme 2. Pathways for Riboflavin (D) Formation Examined in This Investigation ($R = \text{D-Ribityl}$)

Over the past decades, several mechanisms have been proposed; nucleophilic catalysis by a so far unknown nucleophile (Scheme 2, e.g., $\text{XH} = \text{water, serine, or cysteine amino acid side chains}$) was commonly accepted for riboflavin formation.^{4,8} Support for the nucleophilic catalysis mechanism in the enzyme-catalyzed reaction can be derived from the presence of cysteine and histidine in the active site of riboflavin synthase⁶ and because the replacement of these serine or cysteine residues substantially reduces the catalytic activity.⁹ In contrast, it has also been argued on the basis of X-ray crystallographic analysis that the direct involvement of these residues is not very likely.¹⁰

In 2001, Bacher, Fischer, and co-workers isolated the pentacyclic tautomers, B and C, employing an inactive mutant of riboflavin synthase.^{9b} As the native enzyme can catalyze either the forward reaction with formation of the product D or the backward reaction yielding the reactants A, the intermediates B and C can be considered as kinetically competent reaction intermediates. The isolation of these intermediates later inspired the authors to propose another mechanism that requires fewer reaction steps than nucleophilic catalysis and does not require the participation of a catalyst. Their suggestion involves a (6a→7)-hydride transfer (see Scheme 1 for numbering) from the methyl carbon 6a of the lumazine A (or its anion) to the electrophilic position 7 of another lumazine molecule, followed by tautomerization in the dihydrolumazine G and a subsequent inverse-electron-demand Diels–Alder cycloaddition reaction (Scheme 2).¹¹

We have analyzed several conceivable pathways for riboflavin synthesis from 6,7-dimethyl-8-ribityllumazine employing den-

sity functional theory. We now report on the results of these computational studies for the mechanism of nucleophilic catalysis by water or enzyme side chains proposed by Plaut, Wood, and co-workers (Scheme 2) and the hydride transfer and subsequent [4 + 2] cycloaddition pathway suggested by Bacher, Fischer, and co-workers (Scheme 2). We also studied two other mechanisms that were not previously considered, both conceived in Zurich and tested computationally in Los Angeles: a radical pair mechanism that involves a hydrogen atom ($6\text{a}\rightarrow 7\text{a}$)-shift between two lumazine enamine tautomers F to form a radical pair that subsequently collapses through forming a bond between the positions 6a and 7 (Scheme 2). This mechanism would be expected to benefit from the π -conjugative stabilization of the two radicals in the transient radical pair. In a fourth possible mechanism, the enamine form F of one lumazine molecule is converted by a (rate-limiting) proton transfer from methyl position 6a to the diene-enamine tautomer H: The methylidene carbon 6a of this strongly nucleophilic diene undergoes a nucleophilic attack on the electrophilic position 7 of the second lumazine A (Scheme 2). The product of this C–C bond formation is constitutionally prone to undergo the subsequent cyclization step to the pentacycle B with the methylidene carbon 7a acting as the nucleophile. This pathway involves, besides the two strategic C–C bond formations, only intermolecular proton transfers and is expected to benefit strongly from a preorganization of the two reacting lumazine molecules relative to each other for the final C–C-forming step.

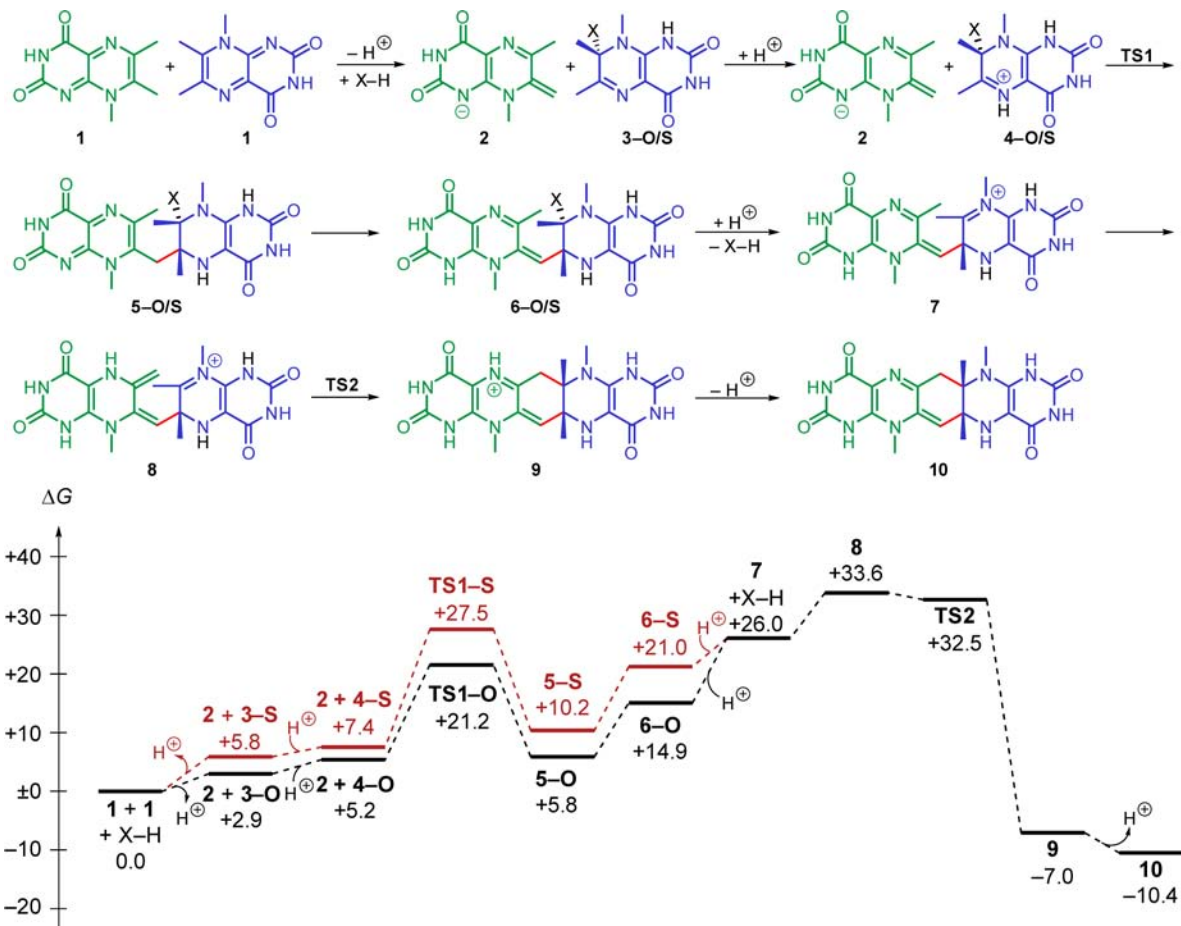


Figure 1. Proposed mechanism and Gibbs energy profiles (in kcal mol⁻¹) for the synthesis of riboflavin via nucleophilic catalysis by water (in black) or by methanethiol (in red) [M06-2X/def2-TZVPP/CPCM//M06-2X/6-31+G(d,p)/IEFPCM].

COMPUTATIONAL DETAILS

The computational analysis of the four mechanisms of riboflavin formation has been carried out with the simplified model 6,7,8-trimethylllumazine in which the ribityl group at position 8 of the natural system is replaced by a methyl group. Structures with the ribityl substituent are numbered with letters, while their methyl analogues are labeled with Arabic numbers.

The conformational space of each intermediate of the proposed mechanisms was searched using the OPLS_2005 force field and a modified Monte Carlo search routine implemented in MACROMODEL 9.9.¹² All structures were subsequently optimized employing M06-2X,¹³ B3LYP,¹⁴ and B3LYP-D2¹⁵ and the double- ζ split-valence 6-31+G(d,p) basis set. Solvation by water was taken into account using the IEFPCM continuum solvation model in both optimization and frequency calculations.¹⁶ It has recently been shown that the presence of a polarizable continuum model does not have a big impact on frequencies, while solvation is sometimes necessary to locate certain transition states that only exist in polar media.¹⁷ Harmonic vibrational frequency calculations verified that each structure was a minimum or a transition state and provided thermal corrections for 298.15 K and 1 mol L⁻¹ (55.5 mol L⁻¹ for H₂O). Following the intrinsic reaction coordinates (IRC) confirmed that all transition states connected the corresponding reactants and products on the potential energy surface. Electronic energies were obtained from single-point calculations employing the M06-2X functional, the large triple- ζ def2-TZVPP basis set, and the CPCM solvation model with UAKS radii.¹⁸ The latter has been shown to reliably compute aqueous solvation free energies for organic compounds.¹⁹ An ultrafine grid was used throughout this study for numerical integration of the density. Entropic contributions to the reported free energies were calculated

from partition functions evaluated using Truhlar's quasiharmonic approximation.¹⁷ This method uses the same approximations as the usual harmonic one except that all vibrational frequencies lower than 100 cm⁻¹ are set equal to 100 cm⁻¹. All computations were performed using Gaussian 09.²⁰

RESULTS AND DISCUSSION

Effects of Functional and Solvation Model. To check the reliability of our calculations, we employed different functionals (M06-2X, B3LYP with and without dispersion correction) in this study. B3LYP energies without Grimme's D2 correction¹⁵ are typically slightly higher compared to the energies obtained from the dispersion-corrected functionals M06-2X and B3LYP-D2. Since calculations using the M06-2X and B3LYP-D2 functionals gave very similar results, the following discussion will be restricted to the M06-2X results.

We also tested several solvation models (IEFPCM, SMD, and CPCM), and all gave the same qualitative picture, although the absolute energies varied between the different models. For the sake of clarity, we will only show the results obtained using the CPCM solvation model.

Nucleophilic Catalysis by Water or a Thiol. In the 1960s, Wood and co-workers proposed a pathway for riboflavin formation that involves nucleophilic catalysis.^{4,8} Due to the occurrence of both cysteine and water in the active site of riboflavin synthase of *Methanocaldococcus jannaschii*,²¹ participation of either of those would seem feasible. The participation of the ribityl substituent as the nucleophilic catalyst is less

likely due to a hydrogen bond network with the protein side chains.²¹ We have calculated Gibbs energy profiles for the nucleophilic catalysis by water and by methanethiol (Figure 1). The latter was chosen to model the cysteine residue within an enzyme active site. The enzyme active site might not be appropriately described by solvation models for water, but for the sake of comparison, we have employed the same solvation model throughout the entire investigation. This also serves as a model for the non-enzymatic process. As both alternative mechanisms proceed with comparable Gibbs energy profiles, the two mechanistic pathways will be discussed together in the next section. The suffixes **-O** and **-S** indicate whether water or methanethiol acts as nucleophilic catalyst.

Due to the relatively high acidity of the lumazine **1** in water ($pK_a = 9.85$),²² proton transfer between the neutral molecule and water is only slightly endergonic. The addition of the nucleophilic catalyst [H_2O or $MeSH$ (Figure 1)] to the lumazine **1** yielding the hemiaminals **3-O** or **3-S** is somewhat endergonic. For both catalysts, a variety of proton transfer reactions involving solvent molecules or, in the enzyme, side chains would be involved in these steps. These transformations increase the electrophilicity at the C-6 carbon atom (see Scheme 1 for numbering) of starting material **1** and promote the attack of the conjugate base **2** of the lumazine **1**. Protonation of the nitrogen at N-5 ($\rightarrow 4-O$ or $4-S$) furthermore increases the reactivities of **3-O/S** and thereby facilitates a nucleophilic attack by **2**. The Gibbs energies of activation (**TS1-O**, +21.2 kcal mol⁻¹; **TS1-S**, +27.5 kcal mol⁻¹, Figure 2) are high, although the overall addition is

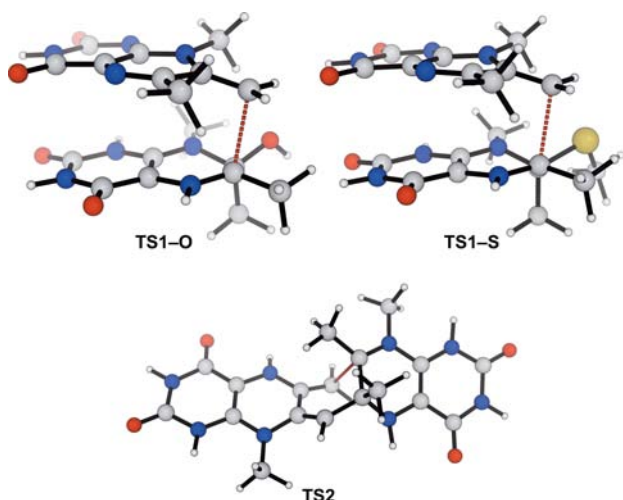


Figure 2. Calculated transition states for the synthesis of riboflavin via nucleophilic catalysis by water or by methanethiol [M06-2X/def-TZVPP/CPCM//M06-2X/6-31+G(d,p)/IEFPCM].

nearly thermoneutral ($\Delta G = +0.6$ kcal mol⁻¹ for H_2O ; +2.8 kcal mol⁻¹ for $MeSH$). The barrier of 16–20 kcal mol⁻¹ is mainly due to the bimolecular reaction that contributes $-T\Delta S$ terms of 14.8 and 15.4 kcal mol⁻¹, respectively. However, the entropic contribution to the activation free energy is probably overestimated due to known problems with the treatment of translational entropy in solution.²³

Formally, these reactions involve the attack of a vinylogous enamine anion on an iminium ion. The corresponding transition states for the attack of **2** on the neutral hemiaminals **3-H** yielding an anionic reaction product were found to be 14

kcal mol⁻¹ higher in energy. The resulting intermediates **5** subsequently isomerize to the corresponding NH tautomers **6**. The intermediates **6-O** and **6-S** are protonated either at the oxygen or sulfur atom of the nucleophilic catalyst and subsequently lose water or methanethiol without an activation barrier to yield the iminium ion **7**.

After another endergonic imine-enamine tautomerization yielding **8**, the six-membered ring is formed in the next step (**TS2**, Figures 1 and 2) by the attack of the enamine on the iminium substructure. A barrier of 1.6 kcal mol⁻¹ between **8** and **TS2** has been calculated on the M06-2X/6-31+G(d,p)/IEFPCM potential energy surface, while negative barriers were obtained from high-level M06-2X single-point calculations. Thus, the conversion of **8** to **9** via **TS2** occurs without a significant barrier. After deprotonation of the resulting iminium ion **9**, the pentacyclic intermediate **10** is obtained which can then be transformed to the final products as discussed later. Steps starting from **6** or **7** and ending at **10** could be afforded in an enzyme by general-acid/general-base catalysis.

Hydride Transfer Mechanism. The mechanism recently proposed by Fischer, Bacher, and co-workers does not assume the participation of an additional nucleophile (Figure 1).¹¹ The key step of this proposal involves the transfer of a hydride ion from the methyl group **6a** of the deprotonated enamine **2** to the electrophilic position **7** of a neutral lumazine molecule **1**. The resulting intermediates **12** and **13**—the latter after tautomerization to **14**—would subsequently undergo a [4 + 2] cycloaddition, yielding the experimentally observed **16**.

As before, deprotonation of **1** is the initial step in the mechanism. Additionally, the second lumazine molecule is protonated at the N1 position to facilitate the transfer of a hydride ion. Such steps in enzyme-catalyzed hydride transfer reactions are often general-acid/general-base-catalyzed.²⁴ Here, the hydride transfer from a lumazine anion **2** to a cationic lumazine **11** was calculated to proceed with the highest barrier within this pathway (**TS3**, $\Delta G^\ddagger = +51.1$ kcal mol⁻¹, Figures 3 and 4). A corresponding transition state for the attack of **2** on a neutral lumazine **1** was located 4.4 kcal mol⁻¹ still higher in energy and is not shown in Figure 3. This barrier is higher than those determined for typical hydride transfer reactions involving NADH ($15 < \Delta G^\ddagger < 25$).^{24,25}

To understand the origin of this unusually high barrier, we additionally calculated the reaction free energies and activation free energies for the hydride transfer reaction to an NAD^+ analogue or from an NADH analogue (Scheme 3). The lumazine anion **2** transfers a hydride anion to the NAD^+ model in an endergonic reaction ($\Delta G = +34.1$ kcal mol⁻¹), while the transfer of a hydride from the NADH analogue to the lumazine cation **11** is exergonic ($\Delta G = -20.6$ kcal mol⁻¹). While the reduction of the conjugated iminium ion **11** proceeds with a typical barrier ($\Delta G^\ddagger = +23.4$ kcal mol⁻¹), the hydride transfer from **2** requires a significantly higher activation barrier ($\Delta G^\ddagger = +52.8$ kcal mol⁻¹). It appears that **2** is kinetically a very poor hydride donor.

Dehydrolumazine **12** and dihydrolumazine **13**, the products of hydride transfer, are less stable than the reactants ($\Delta G = +20.4$ kcal mol⁻¹), and the isomerization of **13** to a suitable dienophile **14** is further endergonic ($\Delta G = +36.1$ kcal mol⁻¹). To verify this large energy difference, we calculated the reaction energy for the reaction of two lumazines **1** to **12** and **14** (Table 1) with a variety of different functionals, basis sets, and solvation models. All methods used for Table 1 show the same high endergonicity for this reaction, presumably due to the

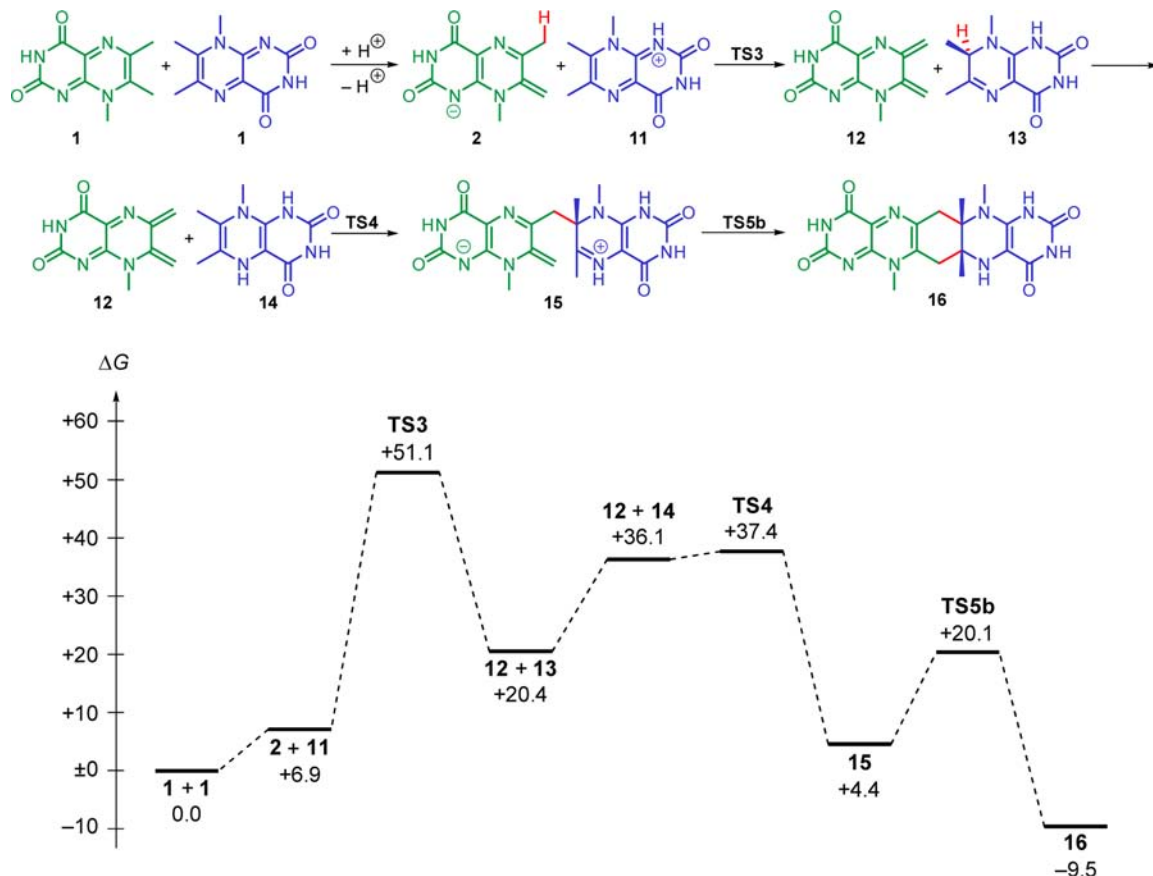


Figure 3. Proposed mechanism and Gibbs energy profiles (in kcal mol⁻¹) for the synthesis of riboflavin via hydride transfer and subsequent cycloaddition [M06-2X/def2-TZVPP/CPCM//M06-2X/6-31+G(d,p)/IEFPCM].

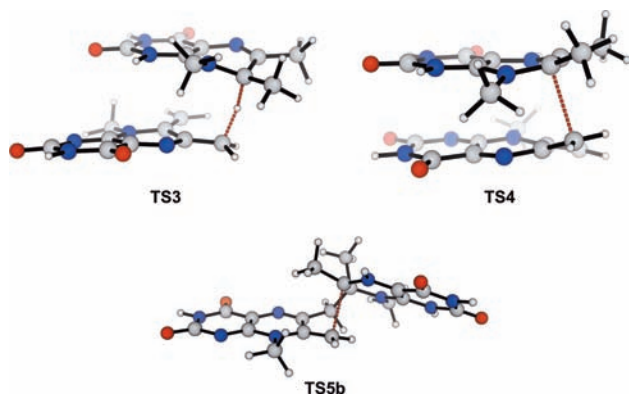


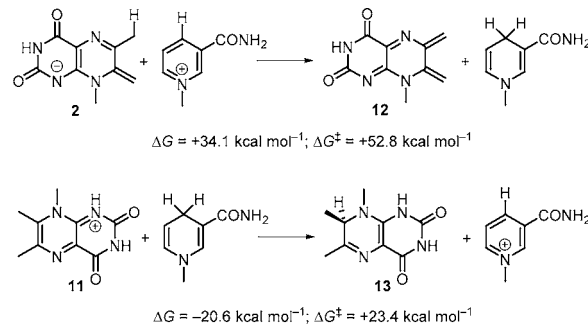
Figure 4. Calculated transition states for the synthesis of riboflavin via the hydride transfer pathway [M06-2X/def2-TZVPP/CPCM//M06-2X/6-31+G(d,p)/IEFPCM].

conversion of 10π electron aromatic **1** to cross-conjugated **12** and 12π antiaromatic **14**.

For the subsequent $[4 + 2]$ cycloaddition, no concerted transition state could be located. The calculations predict a stepwise reaction. The first C–C bond formation is formally the attack of an enamine on an unsaturated imine. It occurs without a significant barrier (TS4, $\Delta G^\ddagger = +37.4$ kcal mol⁻¹, Figures 3 and 4) and yields the zwitterion **15**.

The resulting zwitterionic intermediate **15** can either directly undergo the cyclization step (TS5b, $\Delta G^\ddagger = +20.1$ kcal mol⁻¹, Table 2) or be protonated prior to the ring closing reaction (TS5c, $\Delta G^\ddagger = +20.3$ kcal mol⁻¹, Table 2). The formal attack of

Scheme 3. Reaction Free Energies ΔG and Activation Free Energies ΔG^\ddagger for the Hydride Transfer Reactions between an NADH Analogue and **2 and **11** [M06-2X/def2-TZVPP/CPCM//M06-2X/6-31+G(d,p)/IEFPCM]**



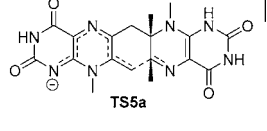
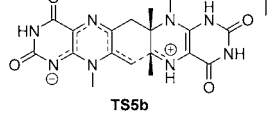
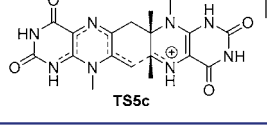
an enamine anion on a neutral imine is too high in energy (TS5a, $\Delta G^\ddagger = +32.5$ kcal mol⁻¹, Table 2) to be considered as an alternative. Transition states for a cyclization reaction of the uncharged neutral isomer **24** (see Figure 8 below) could not be located on the potential energy surface.

The stereochemistry of the observed pentacyclic intermediate **16** has not been determined experimentally. In a computational study using B3LYP/6-31G(d), Zheng and co-workers showed that the *trans* conformation of **16** is preferred over the *cis* conformation in the gas phase by 3.3 kcal mol⁻¹.²⁶ Slightly smaller differences have been calculated for the enzymatic environment ($\varepsilon = 2.02$, $\Delta E = 2.8$ kcal mol⁻¹; and $\varepsilon = 10.65$, $\Delta E = 2.2$ kcal mol⁻¹).

Table 1. Influence of the Computational Method on the Reaction Energies of the Formation of 12 and 14, the Putative Diels–Alder Cycloaddends

method	ΔE^\ddagger (kcal mol ⁻¹)
optimizations employing IEFPCM	
B3LYP/6-31+G(d,p)	+49.0
B3LYP-D2/6-31+G(d,p)	+48.0
M06-2X/6-31+G(d,p)	+46.5
ω B97XD/6-31+G(d,p)	+48.0
MPW1B95/6-31+G(d,p)	+48.6
single points employing CPCM	
B3LYP/6-31+G(d,p)	+42.7
B3LYP-D2/6-31+G(d,p)	+41.8
M06-2X/6-31+G(d,p)	+39.9
ω B97XD/6-31+G(d,p)	+41.9
MPW1B95/6-31+G(d,p)	+42.5
B3LYP/def2-TZVPP	+39.0
B3LYP-D2/def2-TZVPP	+38.1
M06-2X/def2-TZVPP	+36.8
ω B97XD/def2-TZVPP	+38.4
MPW1B95/def2-TZVPP	+39.3

Table 2. Influence of the Protonation State on the Transition State Energies of the First Step of the [4 + 2] Cycloaddition Reaction [Relative to 1a, M06-2X/def2-TZVPP/CPCM//M06-2X/6-31+G(d,p)/IEFPCM]

Transition State	ΔG^\ddagger / kcal mol ⁻¹
	+32.5
	+20.1
	+20.3

Furthermore, docking studies showed that the *trans* pentacycle **trans-16** better fits in the binding pocket of riboflavin synthase than the *cis* isomer **16**.²⁶ Our computations using CPCM ($\epsilon = 78.36$) revealed that in aqueous solution the *cis* and *trans* isomers are isoenergetic (Figure 5). Furthermore, the transition state leading to the *trans* product is much higher in energy ($\Delta\Delta G^\ddagger \approx 20$ kcal mol⁻¹, Figure 5) than the corresponding transition state for the *cis* isomer. Therefore, in aqueous solution, the *cis* pathway will dominate over the *trans* pathway.

Recent experimental^{27a–c} and computational^{27d} studies revealed that a concerted but highly asynchronous [4 + 2] cycloaddition catalyzed by the enzyme SpnF is a key step in the biosynthesis of spinosyn A. Our calculations on the riboflavin

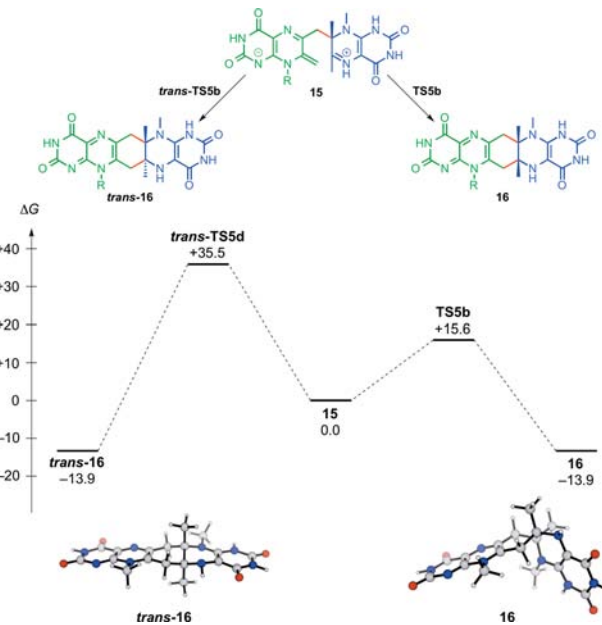


Figure 5. Gibbs energy profile for the *cis* and *trans* cyclization of the zwitterionic intermediate **15** [M06-2X/def2-TZVPP/CPCM//M06-2X/6-31+G(d,p)/IEFPCM].

formation now show that riboflavin synthase cannot be considered as another Diels–Alderase.

Hydrogen Atom Transfer. This mechanism involves a hydrogen atom transfer between two molecules of the enamine form **17** of the lumazine as the key step of riboflavin formation. Whereas in the hydride transfer mechanism the hydrogen would move from position 6a of the donor enamine **17** (or its anion **2**) to position 7 of the acceptor lumazine molecule **17**, in the hydrogen atom transfer mechanism, the hydrogen would move from position 6a of the same enamine but to the position 7a of the acceptor molecule. Both the donor and the acceptor molecules would be the same enamine derivative. The resulting radical pair subsequently would undergo C–C bond formation followed by ring closure to afford the pentacyclic intermediate identical to that obtained in the hydride transfer mechanism.

To elucidate the nature of the hydrogen atom donor and acceptor involved in this pathway, we first explored the diradical character of **1**, by calculating the singlet–triplet energy difference for **1**, its N–H tautomer **17**, and the corresponding anion **2**. True diradicals would have a very low singlet–triplet energy gap. Table 3 shows that in all cases the singlet structures are much more stable than the corresponding triplet structures. The diradical character is found to be small, as reflected in the stability of the restricted solution for the singlet and the large singlet–triplet gap. The tautomer **17**, which is proposed to be involved as an acceptor for a hydrogen atom, is isoenergetic to the C–H tautomer **1**. In **TS6** (Figures 6 and 7), a hydrogen atom is transferred from the lumazine anion **2** to **17**. A hydrogen bond formed between a carbonyl group of the hydrogen atom acceptor and the amide hydrogen of the hydrogen atom donor stabilizes the transition state and is obviously more effective than the dispersion interaction in a perfect parallel orientation of the π systems.

Nevertheless, a very high free energy of activation ($\Delta G^\ddagger = +60.8$ kcal mol⁻¹, Figures 6 and 7) was found for this step. Both an open shell singlet and a triplet were found for this transition state with the singlet being energetically favored by 15 kcal

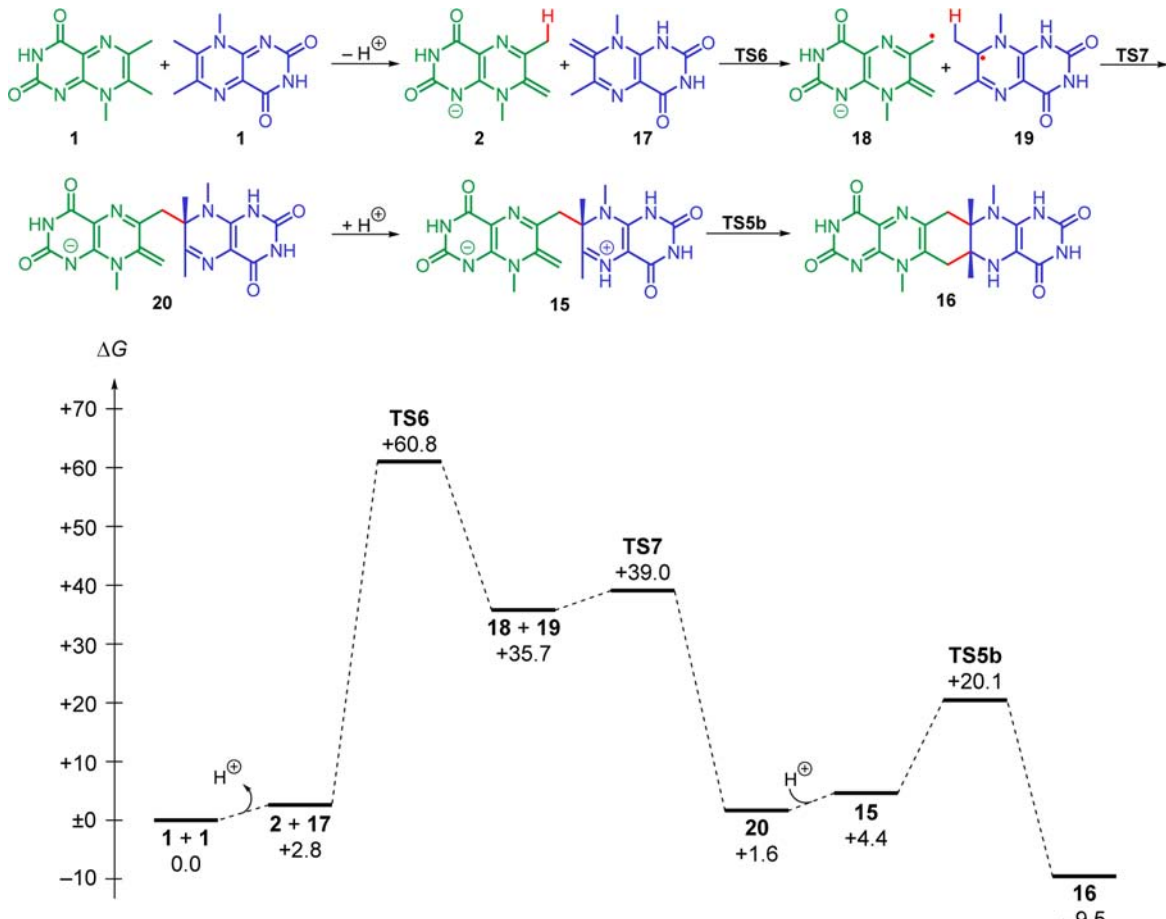


Figure 6. Proposed mechanism and Gibbs energy profiles (in kcal mol⁻¹) for the synthesis of riboflavin via radical pair hydrogen atom transfer and subsequent radical dimerization [M06-2X/def2-TZVPP/CPCM//M06-2X/6-31+G(d,p)/IEFPCM].

Table 3. Differences between the Different Spin States of **1, the N–H Tautomer **17**, and the Anion **2** [ΔΔG in kcal mol⁻¹; M06-2X/def2-TZVPP/CPCM//M06-2X/6-31+G(d,p)/IEFPCM]**

Compound	Singlet (restricted or unrestricted)	Triplet
1a	±0.0	+49.6
17	-0.3	+45.0
2	±0.0	+45.6

mol⁻¹. A change of the protonation state does not yield a lower barrier, and the same energy barrier has been calculated for the hydrogen atom transfer between the lumazine anion **2** and a protonated lumazine tautomer **17-H**.

Typical barriers for the transfer of a hydrogen atom to a carbon-centered radical are 15–30 kcal mol⁻¹,²⁸ while a barrier

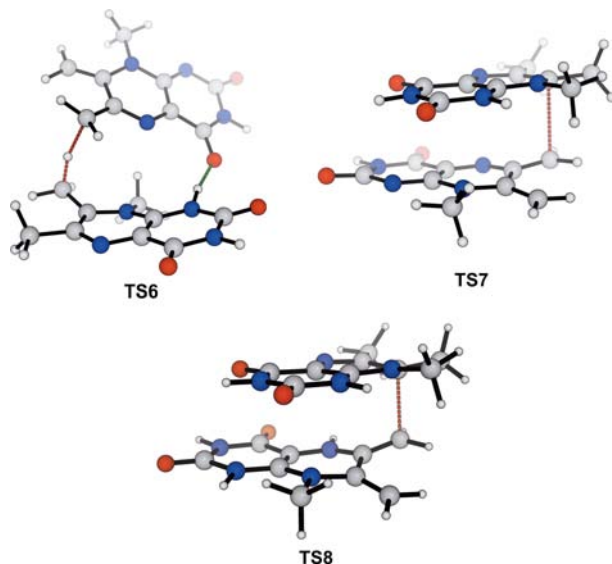
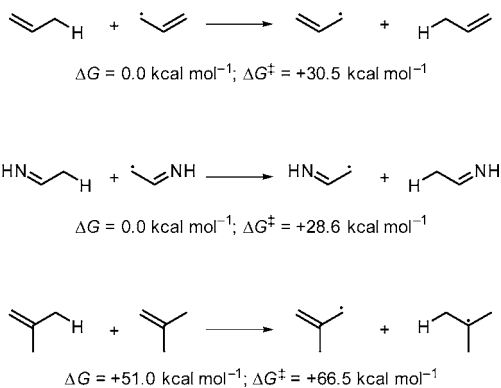


Figure 7. Calculated transition states for the synthesis of riboflavin via the hydrogen atom transfer and the nucleophilic addition pathway [M06-2X/def2-TZVPP/CPCM//M06-2X/6-31+G(d,p)/IEFPCM].

of 58 kcal mol⁻¹ was calculated here for the transfer of a hydrogen atom to a nonradical carbon atom of **17**. To elucidate whether this high barrier is unique to the lumazine system, we calculated the hydrogen atom transfer barriers for three

different model reactions at the same level of theory (Scheme 4). Identity hydrogen atom transfer reactions between propene and the propenyl radical as well as the aza analogues proceed with typical activation energies of about 30 kcal mol⁻¹. In these cases, the $-T\Delta S$ contributions due to the biomolecular reactions are almost identical (ca. 10 kcal mol⁻¹).

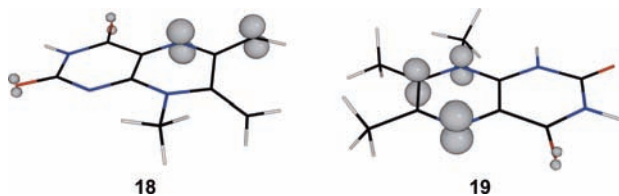
Scheme 4. Reaction Free Energies ΔG and Activation Free Energies ΔG^\ddagger for Different Model Hydrogen Atom Transfer Reactions [M06-2X/def2-TZVPP/CPCM//M06-2X/6-31+G(d,p)/IEFPCM]



In contrast, the activation free energy for the hydrogen atom transfer between isobutene molecules is significantly higher, likely due to the high endergonicity of this reaction. The high barrier for the lumazine system is also likely due to the high endergonicity of the hydrogen atom transfer between non-radical species.

Spin density calculations for the radical products **18** and **19** reveal that the unpaired electron is delocalized within the conjugated π systems and thereby stabilizing the radicals (Scheme 5).

Scheme 5. Spin Density [M06-2X/def2-TZVPP/CPCM//M06-2X/6-31+G(d,p)/IEFPCM] of the Radicals **18 and **19** Obtained from Hydrogen Atom Transfer**

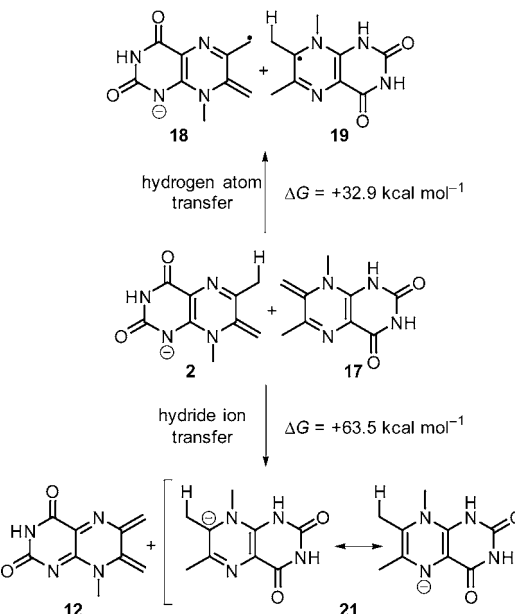


The conceivable closed shell alternative ($\rightarrow \mathbf{12} + \mathbf{21}$, Scheme 6), the transfer of a hydride anion instead of the hydrogen atom, can be excluded as the formed intermediates were found to be an additional 30 kcal mol⁻¹ more endergonic.

The radical pair, **18** and **19**, can now undergo a dimerization reaction to form the upper half of the six-membered ring ($\rightarrow \mathbf{20}$). Only a small activation free energy (3.3 kcal mol⁻¹) was calculated for this step. Again, both an unrestricted singlet and a triplet state were found for the transition state, and the singlet was calculated to be more stable ($\Delta\Delta G = 24$ kcal mol⁻¹). Protonation of the resulting anion ($\rightarrow \mathbf{15}$) is followed by the same cyclization reaction that was discussed above for the hydride transfer mechanism (Figure 4).

Nucleophilic Addition Mechanism. For this mechanism, the enamine tautomer **17** of the lumazine molecule is assumed

Scheme 6. Gibbs Energies for Potential Open Shell Hydrogen Atom or Closed Shell Hydride Ion Transfer [M06-2X/def2-TZVPP/CPCM//M06-2X/6-31+G(d,p)/IEFPCM]



to start the process by undergoing a ketimine-enamine tautomerization to the diene-diamine **22** that acts as nucleophile through the methylidene carbon **6a** in attacking the nucleophilic center **7** of a lumazine molecule, assisted by protonation of N-1 of the latter (Figure 8). The free energy profile of this pathway is shown in Figure 8, and the transition state is depicted in Figure 7.

The transformation of the C–H tautomer **1** to the corresponding N–H tautomer **17** is roughly isoenergetic. In the next step, an endergonic isomerization ($\Delta G = +14.4$ kcal mol⁻¹) of the imine substructure in **17** to the enamine substructure in **22** takes place, while the second lumazine molecule is protonated ($\rightarrow \mathbf{11}$).

The enamine **22** attacks the conjugated iminium ion **11** through transition state **TS8** with an activation free energy of +20.5 kcal mol⁻¹. This exergonic reaction ($\Delta G = -10.8$ kcal mol⁻¹) yields the cation **23**. The corresponding attack on the neutral lumazine **1** is only slightly higher in energy (1 kcal mol⁻¹) but is not shown in Figure 8. Attempts to locate a concerted mechanism for this reaction starting from different transition state guesses failed. The iminium ion **23** is then deprotonated to the neutral **24** before it isomerizes to the zwitterion **15**. This isomerization is necessary for the following cyclization reaction, which has been discussed before (Figure 5). Our computational study predicts that the neutral intermediate **24** does not undergo the second C–C bond formation.

A mechanistic variant is conceivable which would constitute a hybrid between the nucleophilic addition and the nucleophilic catalysis mechanisms. In this pathway, the intermolecular C–C bond formation would again proceed by attack of the nucleophilic methylidene carbon **6a** of an enamine group on the electrophilic center **7** of the lumazine molecule—as is the case in the nucleophilic addition mechanism. However, the enamine that acts as the nucleophile would not be formed from **17**, but rather from **3** (Figure 1), which is the first intermediate

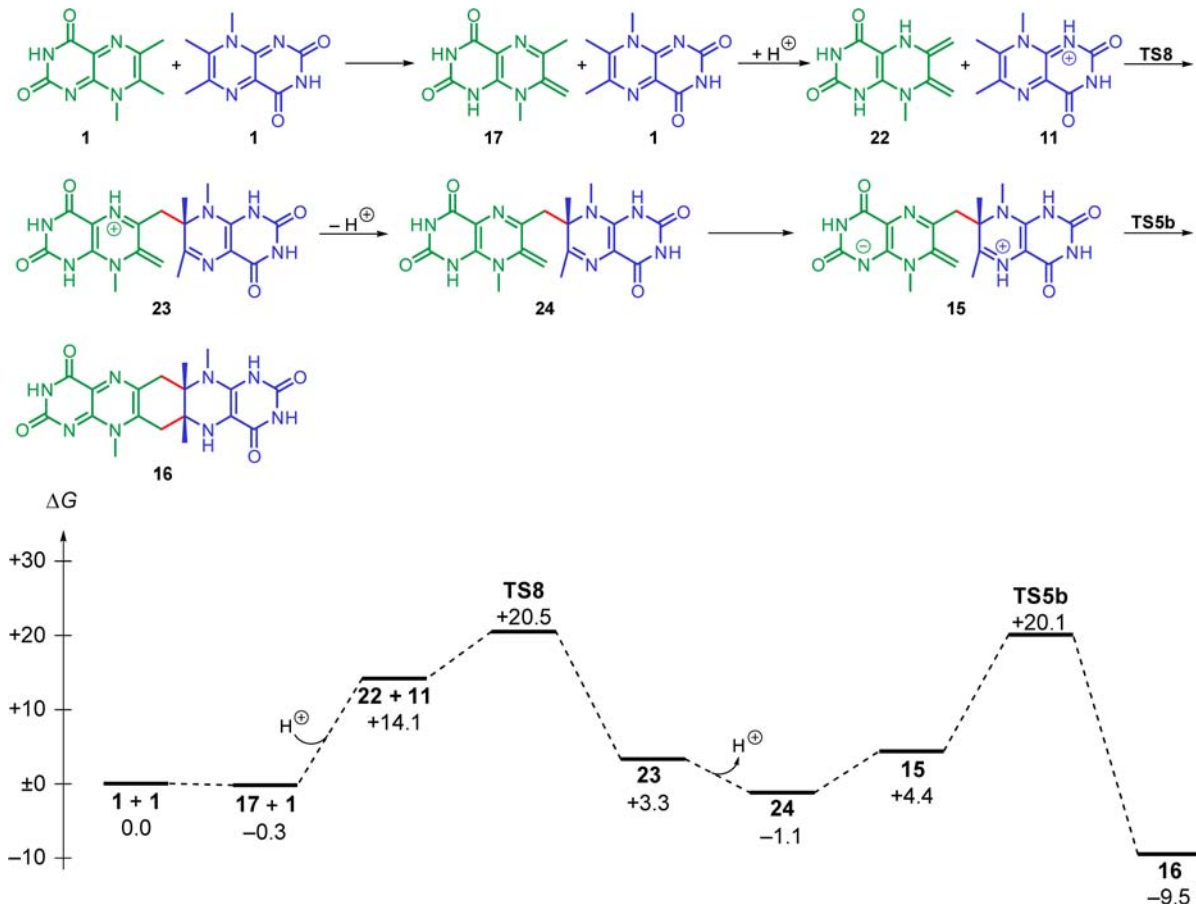
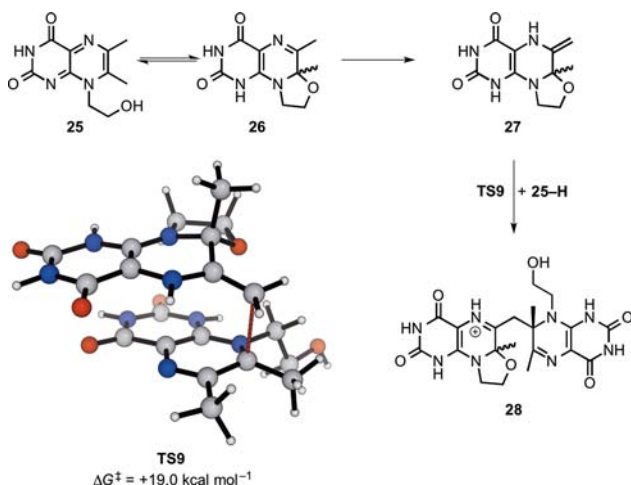


Figure 8. Proposed mechanism and Gibbs energy profiles (in kcal mol^{-1}) for the synthesis of riboflavin via a nucleophilic addition mechanism [M06-2X/def2-TZVPP/CPCM//M06-2X/6-31+G(d,p)/IEFPCM].

in the nucleophilic catalysis mechanism. An alternative possibility involves an intramolecular additions step of the type exemplified by the model system shown in Scheme 7. The finding of Plaut and co-workers,⁴ according to which the methyl group 6a in a dihydro derivative of lumazine 1 (e.g., 13 in Scheme 3 and Figure 3) exchanges protons under deuteration

Scheme 7. Transition State Model for the Direct Participation of the Ribityl Group in the Nucleophilic Addition Ion Transfer [M06-2X/def2-TZVPP/CPCM//M06-2X/6-31+G(d,p)/IEFPCM]



conditions and lends support to such a variant. The intermediates along this pathway either are identical (intermediates 3, 11, and 24) or have structures closely analogous to intermediates of calculated pathways (Figures 1, 3, and 8), and all would be low in energy. For the simple model system depicted in Scheme 7, we calculated a very similar yet slightly smaller barrier for the initial C–C bond formation, involving TS9 shown in Scheme 7.

Conversion of the Pentacyclic Intermediates to Riboflavin. The final steps of the riboflavin formation, that is, transformation of the pentacyclic intermediates via 29 to the riboflavin analogue, 30, and 5-amino-6-(methylamino)uracil, 31, is the same for all pathways discussed above. While the intermediates from the hydride transfer, the radical pair mechanism, and the nucleophilic addition mechanisms enter these final transformations in the first stage with 16, the intermediate 10 is already obtained as the product of the nucleophilic catalysis pathway (Figure 9). All of these transformations mainly consist of isomerization or deprotonation/reprotonation reactions and are driven by the highly exergonic ($\Delta G = -29.9 \text{ kcal mol}^{-1}$) overall reaction. We have not attempted to compute the proton transfer steps but show the energies of intermediates in Figure 9.

All compounds depicted in Figure 9 are much lower in energy than the highest intermediates involved in the mechanisms described above. Furthermore, all intermediates formed in the proposed mechanisms have to undergo the same final transformations.

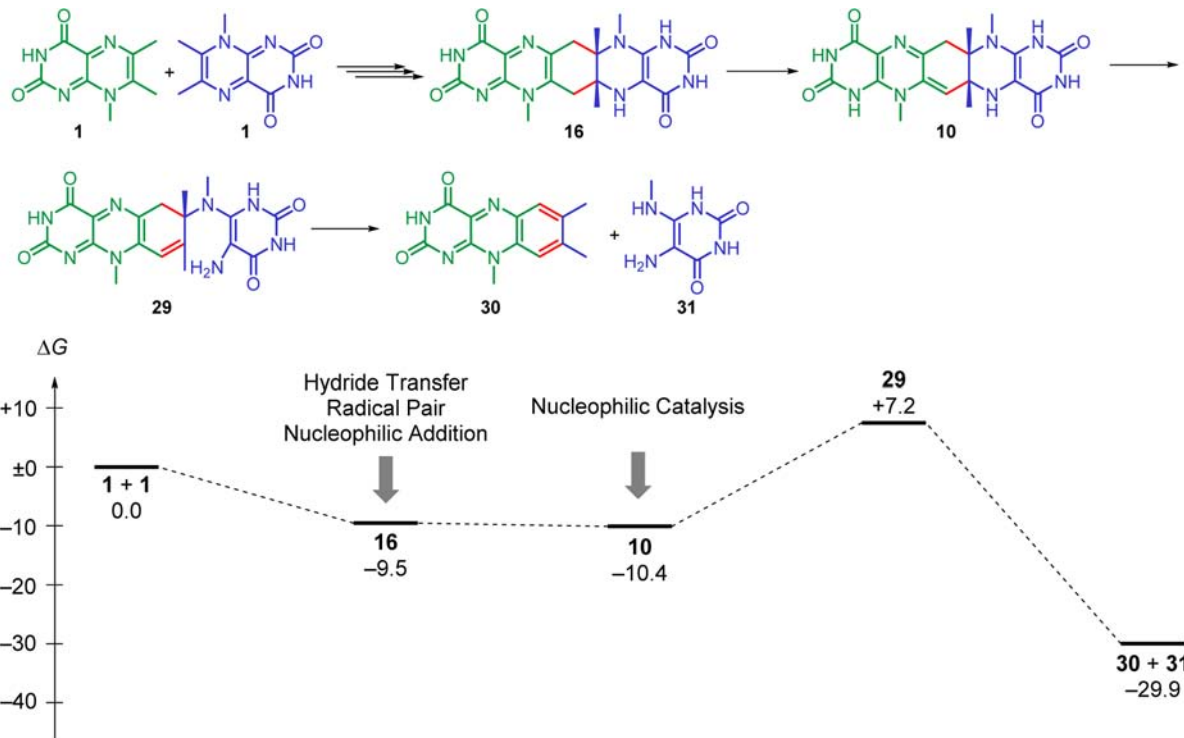


Figure 9. Proposed Gibbs energy profiles (in kcal mol^{-1}) for the conversion of the pentacyclic intermediates **10** and **16** to riboflavin (**30**) [M06-2X/def2-TZVPP/CPCM//M06-2X/6-31+G(d,p)/IEFPCM].

CONCLUSIONS

We have analyzed four different conceivable pathways of riboflavin formation (nucleophilic catalysis, hydride transfer plus Diels–Alder, hydrogen atom transfer, and a nucleophilic addition of an enamine intermediate) by means of density functional theory. Comparing the Gibbs energy profiles in Figures 1, 3, 6, 8, and 9, we conclude that both the hydride transfer (rate-limiting step: TS3, $+51.1 \text{ kcal mol}^{-1}$, Figure 3) and the transfer of a hydrogen atom (TS6, $+60.8 \text{ kcal mol}^{-1}$, Figure 6) are $30\text{--}45 \text{ kcal mol}^{-1}$ higher in energy than the nucleophilic addition mechanism, which was calculated as the lowest energy pathway.

The main reasons for these unfavorable barriers are the high-energy intermediates in these pathways. The hydride transfer mechanism involves a highly electrophilic diene system as intermediate, formally prone to subsequently undergo a Diels–Alder addition. However, it is found that a concerted Diels–Alder reaction between the intermediates **12** and **14** does not take place, and that the coupling of the two species would occur by a stepwise mechanism. Riboflavin synthase is not to be considered another Diels–Alderase.

The mechanism involving nucleophilic catalysis is 13 kcal mol^{-1} higher in energy than the lowest energy pathway, which renders nucleophilic catalysis unlikely at least for the reaction in hot water.

This study shows that, from the point of view of our theoretical analysis, the nucleophilic addition mechanism is the preferred pathway of riboflavin formation for the reaction in hot water. Arguments in favor of the possibility that it may also be the pathway of the enzymatic reaction include the following: The mechanism is perfectly in line with the large isotope effect observed for the enzymatic riboflavin formation, according to which the removal of the hydrogen from the methyl position 6a is rate-limiting.⁴ The mechanism is constitutionally simple and

does not require any chemical assistance except proton transfers from and to the environment. The calculated constellation of the two acting lumazine units in the transition state (see Figure 7) seems to be compatible with what is known of the active site of the enzyme.²¹

There are contradicting views in the literature whether a cysteine residue of the enzyme may be competent to participate in nucleophilic catalysis of the enzyme-catalyzed reaction.^{9,10} Because of this uncertainty, the pathway via nucleophilic catalysis cannot be excluded. Neither can the variant be excluded that is a hybrid between the nucleophilic addition and the nucleophilic catalysis mechanism. Close proximity of water or the cysteine side chain within the enzyme active site might change the energy values and inter-relationships in the calculated energy profile of the nucleophilic catalysis mechanism. The nucleophilic addition mechanism has the potential to win out against other mechanisms in the environment of an enzyme. This adds an important competitor to the mechanistic spectrum of riboflavin formation. The reaction profiles calculated for the hydride shift and the radical pair mechanism rule out these two mechanistic variants.

ASSOCIATED CONTENT

S Supporting Information

Cartesian coordinates and energies of all reported structures, and details of computational methods. This material is available free of charge via the Internet at <http://pubs.acs.org>.

AUTHOR INFORMATION

Corresponding Author

houk@chem.ucla.edu; eschenmoser@org.chem.ethz.ch

Notes

The authors declare no competing financial interest.

ACKNOWLEDGMENTS

We are grateful to the Alexander von Humboldt Foundation (Feodor Lynen scholarship to M.B.) and the National Science Foundation (CHE-0548209 to K.N.H.) for financial support of this research. This work used the Extreme Science and Engineering Discovery Environment (XSEDE), which is supported by National Science Foundation Grant No. OCI-1053575, and resources from the UCLA Institute for Digital Research and Education (IDRE). We thank Steven V. Jerome for preliminary calculations.

REFERENCES

- (1) Plaut, G. W. *E. J. Biol. Chem.* **1960**, *235*, PC41–PC42.
- (2) Plaut, G. W. *E. J. Biol. Chem.* **1963**, *238*, 2225–2243.
- (3) Wacker, H.; Harvey, R. A.; Winestock, C. H.; Plaut, G. W. *E. J. Biol. Chem.* **1964**, *239*, 3493–3497.
- (4) Plaut, G. W. E.; Beach, R. L.; Aogaichi, T. *Biochemistry* **1970**, *9*, 771–785.
- (5) (a) Rowan, T.; Wood, H. C. S. *Proc. Chem. Soc.* **1963**, 21–22. (b) Beach, R.; Plaut, G. W. E. *Tetrahedron Lett.* **1969**, *10*, 3489–3492. (c) Paterson, T.; Wood, H. C. S. *J. Chem. Soc. D* **1969**, 290–291. (d) Paterson, T.; Wood, H. C. S. *J. Chem. Soc., Perkin Trans. 1* **1972**, 1051–1056.
- (6) Truffault, V.; Coles, M.; Diercks, T.; Abelmann, K.; Eberhardt, S.; Lüttgen, H.; Bacher, A.; Kessler, H. *J. Mol. Biol.* **2001**, *309*, 949–960.
- (7) (a) Neuberger, G.; Bacher, A. *Biochem. Biophys. Res. Commun.* **1985**, *127*, 175–181. (b) Talukdar, A.; Zhao, Y.; Lv, W.; Bacher, A.; Illarionov, B.; Fischer, M.; Cushman, M. *J. Org. Chem.* **2012**, *77*, 6239–6261.
- (8) Rowan, T.; Wood, H. C. S. *J. Chem. Soc. C* **1968**, 452–458.
- (9) (a) Gerhardt, S.; Schott, A.-K.; Kairies, N.; Cushman, M.; Illarionov, B.; Eisenreich, W.; Bacher, A.; Huber, R.; Steinbacher, S.; Fischer, M. *Structure* **2002**, *10*, 1371–1381. (b) Illarionov, B.; Eisenreich, W.; Bacher, A. *Proc. Natl. Acad. Sci. U.S.A.* **2001**, *98*, 7224–7229.
- (10) Illarionov, B.; Haase, I.; Bacher, A.; Fischer, M.; Schramek, N. *J. Biol. Chem.* **2003**, *278*, 47700–47706.
- (11) Kim, R.-R.; Illarionov, B.; Joshi, M.; Cushman, M.; Lee, C. Y.; Eisenreich, W.; Fischer, M.; Bacher, A. *J. Am. Chem. Soc.* **2010**, *132*, 2983–2990.
- (12) *MacroModel*, version 9.9; Schrödinger, LLC: New York, 2012.
- (13) Zhao, Y.; Truhlar, D. *Theor. Chem. Acc.* **2008**, *120*, 215–241.
- (14) (a) Becke, A. D. *J. Chem. Phys.* **1993**, *98*, 5648–5652. (b) Lee, C.; Yang, W.; Parr, R. G. *Phys. Rev. B* **1988**, *37*, 785–789.
- (15) Grimme, S. *J. Comput. Chem.* **2006**, *27*, 1787–1799.
- (16) Cancès, E.; Mennucci, B.; Tomasi, J. *J. Chem. Phys.* **1997**, *107*, 3032–3041.
- (17) Ribeiro, R. F.; Marenich, A. V.; Cramer, C. J.; Truhlar, D. G. *J. Phys. Chem. B* **2011**, *115*, 14556–14562.
- (18) (a) Klamt, A.; Schüürmann, G. *J. Chem. Soc., Perkin Trans. 2* **1993**, 799–805. (b) Andzelm, J.; Kölmel, C.; Klamt, A. *J. Chem. Phys.* **1995**, *103*, 9312–9320. (c) Barone, V.; Cossi, M. *J. Phys. Chem. A* **1998**, *102*, 1995–2001. (d) Cossi, M.; Rega, N.; Scalmani, G.; Barone, V. *J. Comput. Chem.* **2003**, *24*, 669–681.
- (19) Takano, Y.; Houk, K. N. *J. Chem. Theory Comput.* **2005**, *1*, 70–77.
- (20) Frisch, M. J.; Trucks, G. W.; Schlegel, H. B.; Scuseria, G. E.; Robb, M. A.; Cheeseman, J. R.; Scalmani, G.; Barone, V.; Mennucci, B.; Petersson, G. A.; Nakatsuji, H.; Caricato, M.; Li, X.; Hratchian, H. P.; Izmaylov, A. F.; Bloino, J.; Zheng, G.; Sonnenberg, J. L.; Hada, M.; Ehara, M.; Toyota, K.; Fukuda, R.; Hasegawa, J.; Ishida, M.; Nakajima, T.; Honda, Y.; Kitao, O.; Nakai, H.; Vreven, T.; Montgomery, J. A., Jr.; Peralta, J. E.; Ogliaro, F.; Bearpark, M.; Heyd, J. J.; Brothers, E.; Kudin, K. N.; Staroverov, V. N.; Kobayashi, R.; Normand, J.; Raghavachari, K.; Rendell, A.; Burant, J. C.; Iyengar, S. S.; Tomasi, J.; Cossi, M.; Rega, N.; Millam, J. M.; Klene, M.; Knox, J. E.; Cross, J. B.; Bakken, V.; Adamo, C.; Jaramillo, J.; Gomperts, R.; Stratmann, R. E.; Yazyev, O.; Austin, A. J.; Cammi, R.; Pomelli, C.; Ochterski, J. W.; Martin, R. L.; Morokuma, K.; Zakrzewski, V. G.; Voth, G. A.; Salvador, P.; Dannenberg, J. J.; Dapprich, S.; Daniels, A. D.; Farkas, Ö.; Foresman, J. B.; Ortiz, J. V.; Ciosowski, J.; Fox, D. J. *Gaussian 09*, revision C.01; Gaussian, Inc.: Wallingford, CT, 2009.
- (21) Ramsperger, A.; Augustin, M.; Schott, A.-K.; Gerhardt, S.; Krojer, T.; Eisenreich, W.; Illarionov, B.; Cushman, M.; Bacher, A.; Huber, R.; Fischer, M. *J. Biol. Chem.* **2006**, *281*, 1224–1232.
- (22) McAndless, J. M.; Stewart, R. *Can. J. Chem.* **1970**, *48*, 263–270.
- (23) (a) Mammen, M.; Shakhnovich, E. I.; Deutch, J. M.; Whitesides, G. M. *J. Org. Chem.* **1998**, *63*, 3821–3830. (b) Straobl, M.; Sham, Y. Y.; Villà, J.; Chu, Z.-T.; Warshel, A. *J. Phys. Chem. B* **2000**, *104*, 4578–4584. (c) Zhou, H.-X.; Gilson, M. K. *Chem. Rev.* **2009**, *109*, 4092–4107.
- (24) (a) Nagel, Z. D.; Klinman, J. P. *Chem. Rev.* **2006**, *106*, 3095–3118. (b) Hammes, G. G.; Benkovic, S. J.; Hammes-Schiffer, S. *Biochemistry* **2011**, *50*, 10422–10430. (c) McGeagh, J. D.; Ranaghan, K. E.; Mulholland, A. J. *Biochim. Biophys. Acta* **2011**, *1814*, 1077–1092. (d) Haines, B. E.; Steussy, C. N.; Stauffacher, C. V.; Wiest, O. *Biochemistry* **2012**, *51*, 7983–7995.
- (25) (a) Wu, Y. D.; Houk, K. N. *J. Am. Chem. Soc.* **1987**, *109*, 906–908. (b) Wu, Y. D.; Houk, K. N. *J. Am. Chem. Soc.* **1991**, *113*, 2353–2358. (c) Wu, Y.-D.; Lai, D. K. W.; Houk, K. N. *J. Am. Chem. Soc.* **1995**, *117*, 4100–4108.
- (26) Zheng, Y.-J.; Jordan, D. B.; Liao, D.-I. *Bioorg. Chem.* **2003**, *31*, 278–287.
- (27) (a) Kim, H. J.; Ruszczycky, M. W.; Choi, S.-h.; Liu, Y.-n.; Liu, H.-w. *Nature* **2011**, *473*, 109–112. (b) Kelly, W. L. *Nature* **2011**, *473*, 35–36. (c) Kim, H. J.; Ruszczycky, M. W.; Liu, H.-w. *Curr. Opin. Chem. Biol.* **2012**, *16*, 124–131. (d) Hess, B. A., Jr.; Smentek, L. *Org. Biomol. Chem.* **2012**, *10*, 7503–7509.
- (28) (a) Camaiione, D. M.; Autrey, S. T.; Salinas, T. B.; Franz, J. A. *J. Am. Chem. Soc.* **1996**, *118*, 2013–2022. (b) Dybala-Defratyka, A.; Paneth, P.; Pu, J.; Truhlar, D. G. *J. Phys. Chem. A* **2004**, *108*, 2475–2486.